J Comput Aided Mol Des (2008) 22:925–933
DOI 10.1007/s10822-008-9229-0

Molecular dynamics simulation study of PTP1B with allosteric inhibitor and its application in receptor based pharmacophore modeling

Kavitha Bharatham · Nagakumar Bharatham · Yong Jung Kwon · Keun Woo Lee

Received: 31 January 2008 / Accepted: 8 July 2008 / Published online: 7 August 2008

Abstract Allosteric inhibition of protein tyrosine phosphatase 1B (PTP1B), has paved a new path to design specific inhibitors for PTP1B, which is an important drug target for the treatment of type II diabetes and obesity. The $PTP1B_{1–282}$-allosteric inhibitor complex crystal structure lacks α7 (287–298) and moreover there is no available 3D structure of $PTP1B_{1–298}$ in open form. As the interaction between α7 and α6–α3 helices plays a crucial role in allosteric inhibition, α7 was modeled to the $PTP1B_{1–282}$ in open form complexed with an allosteric inhibitor (compound-2) and a 5 ns MD simulation was performed to investigate the relative orientation of the α7–α6–α3 helices. The simulation conformational space was statistically sampled by clustering analyses. This approach was helpful to reveal certain clues on PTP1B allosteric inhibition. The simulation was also utilized in the generation of receptor based pharmacophore models to include the conformational flexibility of the protein-inhibitor complex. Three cluster representative structures of the highly populated clusters were selected for pharmacophore model generation. The three pharmacophore models were subsequently utilized for screening databases to retrieve molecules containing the features that complement the allosteric site. The retrieved hits were filtered based on certain drug-like properties and molecular docking simulations were performed in two different conformations of protein. Thus, performing MD simulation with α7 to investigate the changes at the allosteric site, then developing receptor based pharmacophore models and finally docking the retrieved hits into two distinct conformations will be a reliable methodology in identifying PTP1B allosteric inhibitors.

Keywords PTP1B · Allosteric inhibition · Molecular dynamics simulation · Cluster analysis · Receptor based pharmacophore model · Database screening · GOLD molecular docking

Introduction

The protein tyrosine phosphatase 1B (PTP1B) is an attractive target for therapeutic intervention as it is a negative regulator of insulin/leptin receptor phosphorylation and signaling [1, 2]. It is emerging as an important drug target for the treatment of type II diabetes and obesity [3–5] by small molecule inhibitors [6]. PTP1B belongs to nontransmembrane, intracellular PTP superfamily which is characterized by a single catalytic PTP domain flanked by N- or C-terminal motif that localizes the protein to specific subcellular localizations [7]. The catalytic PTP domain of PTP1B shares 72% sequence identity with its closely related TCPTP unlike other phosphatases [8]. Therefore the inhibitors that target PTP1B with identified selectivity determinants at catalytic site are generally selective over most other PTPs [9, 10] tested but are equipotent on T-cell protein tyrosine phosphatase (TCPTP) [11]. Moreover, selective PTP1B inhibitors with acceptable pharmacological properties like cell membrane permeability and bioavailability have proven to be extremely difficult due to the closed form of the catalytic site of PTP1B

Electronic supplementary material The online version of this article (doi:10.1007/s10822-008-9229-0) contains supplementary material, which is available to authorized users.

K. Bharatham · N. Bharatham · K. W. Lee (✉)
Division of Applied Life Science (BK21 Program),
Environmental Biotechnology National Core Research Center,
Gyeongsang National University, Jinju 660-701, Korea
e-mail: kwlee@gnu.ac.kr

Y. J. Kwon
Department of Chemical Engineering,
Kangwon National University, Chunchon 200-701, Korea

containing a highly polar phosphotyrosine (pTyr) binding site [12]. Although derivatives of benzbromarone discovered by high-throughput screening were suspected to exert their inhibitory effect distal from the active site of PTP1B [13], it was not until these compounds were crystallized with PTP1B that a new regulatory site was identified. In 2004, Wiesmann et al. discovered an allosteric site approximately 20 Å away from the catalytic pocket. This has paved a new path to design inhibitors for PTP1B with reasonable pharmacological properties and selectivity as this site is poorly conserved amongst phosphatases and with TC-PTP specifically, as a cysteine is present instead of phenylalanine at the central position 280 of PTP1B [14].

Crystallographic studies have shown that PTP1B can exist in two conformations. In the native, un-liganded form, the WPD-loop is in an ''open'' conformation, and the binding pocket is easily accessible to substrate. Upon substrate binding, the WPD-loop closes over the active site, forming a tight binding pocket for the substrate [15, 16]. The WPD-loop closure is essential for the catalytic mechanism of PTP1B [17]. It is believed that allosteric inhibitors act by stabilizing a conformation that precludes the closure of the WPD-loop in part, by blocking the interaction between α7 and α3–α6 [14]. It is also known that PTP1B inhibitor-resistant mutations were found to concentrate on helix α7 and its surrounding region, but not in the active site [18]. These evidences strongly indicate the role of α7 in allosteric inhibition and also in the open–close transition of WPD-loop.

In a recent study molecular dynamics (MD) and targeted molecular dynamics (tMD) simulations of PTP1B with α7 and one of Wiesmann's inhibitors were performed to understand the WPD-loop movement from open to close form. They examined the behavior of the α3-helix during both MD and tMD simulations. It was concluded that allosteric inhibitor reduced the mobility of the WPD-loop and S-loop (residues 198–209) [19, 20]. However, our aim is to investigate the molecular level interactions between the allosteric inhibitor and PTP1B allosteric site specifically with α7 by MD simulation studies. The MD simulations in general consider the protein's flexibility by generating an ensemble of protein conformations that will be useful in the pharmacophore development and hence it was taken advantage in developing receptor based pharmacophore model. Developing a pharmacophore model considering the conformational changes in the site is logical and will increase the reliability of the models [21]. These receptor based pharmacophore models were used to screen databases in retrieving hits which would possess all the required features to interact with the allosteric site. The hits will be filtered and docked into the allosteric site of two structures representing different conformations. Their binding orientation with respect to the conformational changes at the allosteric site will also be contemplated. This methodology will be useful in identifying new PTP1B allosteric inhibitors with similar binding orientation as existing compounds.

Methods

Molecular dynamics (MD) simulations

The crystal structure of PDBID:1T49 ($PTP1B_{1–282}$) was taken for MD simulation calculations as it contains the allosteric inhibitor. The α7 helix structure was built using the closed form PTP1B crystal structure (PDBID:1SUG) to generate $PTP1B_{1–298}$ structure. In this work we would like to follow the observations made by kamerlin et al. that the residues 282–286 represent the loop between α6 and α7 and the residues 287–295 represent α7 helix. Three 5 ns MD simulations were performed with GROMACS forcefield using *GROMACS 3.3.1* package [22, 23] on a high performance linux cluster computer. Initially, protonation states were added for all the ionizable residues in the protein at a pH 7 and the C-terminal (–COOH) was neutral as it is not the real terminus to avoid artifacts. The topology files and charges for the ligand atoms were calculated using the PRODRG web-server [24]. A protein-ligand complex was inserted into a water box of 1.2 nm from the surface of the protein. The system was neutralized with counter-ions and energy minimization was performed using steepest descent for 1,000 steps. Then the protein backbone was frozen and the solvent molecules with counter-ions were allowed to move during a 50 ps position restrained MD run. Finally 5 ns production run was performed with the simulation period chosen as a compromise between the quality of configuration space sampling and the calculation length. The electrostatic interactions were calculated by the PME algorithm, with interpolation order of 4 and a grid spacing of 0.12 nm. All simulations were run under periodic boundary conditions with NPT ensemble using Berendsen's coupling algorithm for keeping the temperature (300 K) and the pressure (1 bar) constant. The *SHAKE* algorithm with a tolerance of 10–5 Å was applied to fix all bonds containing hydrogen atoms. The time step for the simulations was 2 fs and the coordinates were stored every 1 ps. The van der Waals (vdw) forces were treated by using a cutoff of 12 Å. All the analyses of the trajectory were performed by *GROMACS 3.3.1* program.

Selection of representative snapshots

From a total of 5000 frames saved during the MD simulation, selection of few representative snapshots which could represent the conformational flexibility of the protein is crucial. Therefore, *g_cluster* analyses included with the

GROMACS distribution was used for cluster analysis of the trajectory. First an XPM matrix file is generated with the root mean-square deviation (RMSD) comparisons of each snapshot with all the others. Ten clusters were generated by single linkage method in which a structure is added to a cluster when its distance to any element of the cluster is less than a cutoff of 0.06 nm.

Structure based pharmacophore model generation

Feature mapping module present in *Discovery Studio* program [25] was used to map all the crucial features present in compound-2 for the cluster representative conformations. The features considered were H-bond donor (HBD), H-bond acceptor (HBA), ring aromatic (RA), and hydrophobic (HY) features. A six feature pharmacophore model was chosen based on the crucial interactions maintained by the allosteric inhibitor. Therefore, pharmacophore model that complements the protein's active site is developed by considering the receptor's flexibility. As each pharmacophore model is developed based on the direction of interactions of compound-2 with $PTP1B_{1–298}$ allosteric site it is referred as receptor based pharmacophore model. As cluster six (16.64), eight (29.4) and ten (36.34) together included 82.38% of the MD simulation conformational space, they were taken for further studies. The three receptor based pharmacophore models were used to screen NCI2000 and Maybridge databases to retrieve hits using *CATALYST* software [26].

Molecular docking studies

Evaluation of the binding orientations of compounds retrieved by receptor based pharmacophore models was performed using *GOLD* molecular docking. The *GOLD 3.0.1* program (Genetic Optimisation for Ligand Docking) [27], from Cambridge Crystallographic Data Center, UK, uses a genetic algorithm for docking flexible ligands into protein binding sites. The ligand molecules were docked into two different conformations of $PTP1B_{1–298}$ allosteric site (initial and cluster 10 representative structures) with a radius of 5.0 Å around the crystal ligand. The RMSD, annealing parameter of vdw interaction and hydrogen bond interaction were considered within 1.5, 4.0 and 2.5 Å, respectively.

Results and discussion

MD simulation studies

The crystal structure of $PTP1B_{1–282}$ with compound-2 (PDBID:1T49) at the allosteric site is considered for our studies. The α7 helix is disordered and there is no other available PTP1B 3D structure in open form with α7. The prevention of the interaction between α7 and α3–α6 is supposed to be hindering the transition from open to closed form of PTP1B. Moreover, activity decrease was observed in the α7 truncated PTP1B suggesting the crucial role of α7 in full enzyme activity [14]. Owing to the importance of α7 in allosteric inhibition, it was modeled to the structure of PDBID:1T49 and was taken as an initial structure for MD simulation studies. Two simulations of $PTP1B_{1–298}$ with and without compound-2 were performed for 5 ns as the system was stabilized with no prominent changes after 4 ns. The stability of $PTP1B_{1–298}$ with compound-2 was evaluated based on the analyses of the root mean square deviation (RMSD) and the total energy of the protein. Both the analyses have revealed that the system was stabilized thus confirming that the simulation is reliable with no artifacts (Fig. 1a and b). It was hypothesized that the compound-2 occupies the site of Trp291 and thus stabilizes in the groove formed between the α7 and α3–α6 helices thereby blocking their interaction [14]. Our simulation results also demonstrate that the orientation of the compound-2 remained in such a way during the simulation time that the benzofuran was stacked between the side chains of Trp291 and Leu192. The benzofuran core is in a hydrophobic pocket formed by Trp291, Phe280, Phe196 and Leu192 (Fig. 1c). This can be observed by measuring the minimum distance between the compound-2 and the four residues throughout the simulation (Fig. 1d). The average minimum distance between Trp291, Phe280, Phe196 and Leu192 and the compound-2 were 0.26, 0.33, 0.33 and 0.33 nm respectively. The Pro188 which also interacts with the inhibitor is also within 0.27 nm distance throughout. These hydrophobic interactions stabilize the inhibitor in the α7–α3–α6 groove.

The simulation with compound-2 was further analyzed by clustering the snapshots based on the RMSDs of atom positions wherein each structure is added to a cluster when its distance to any element of the cluster is less than a certain cutoff. This analysis will be useful to statistically characterize conformational families which are sampled during the simulations. Ten clusters (Fig. 2a) were obtained with a cutoff of 0.06 nm and each cluster has a representative structure. This analysis helped us to inspect the changes occurring in α7 helix and the allosteric inhibitor/compound-2 with respect to α3–α6 helices. When four among ten cluster representative structures (Fig. 2b) were superimposed, an upward movement of α7 helix along with a part of the loop (between α6 and α7 helices) was clearly noticeable. Although the α3 and α6 helices aligned perfectly, the residues from Ser285–Leu294 have moved 0.6–0.8 nm upwards. This can be observed clearly by measuring and comparing the distance between Glu200 (residue of α3)-Met282 (residue of α6) and Glu200–Val287 (residue of α7) in

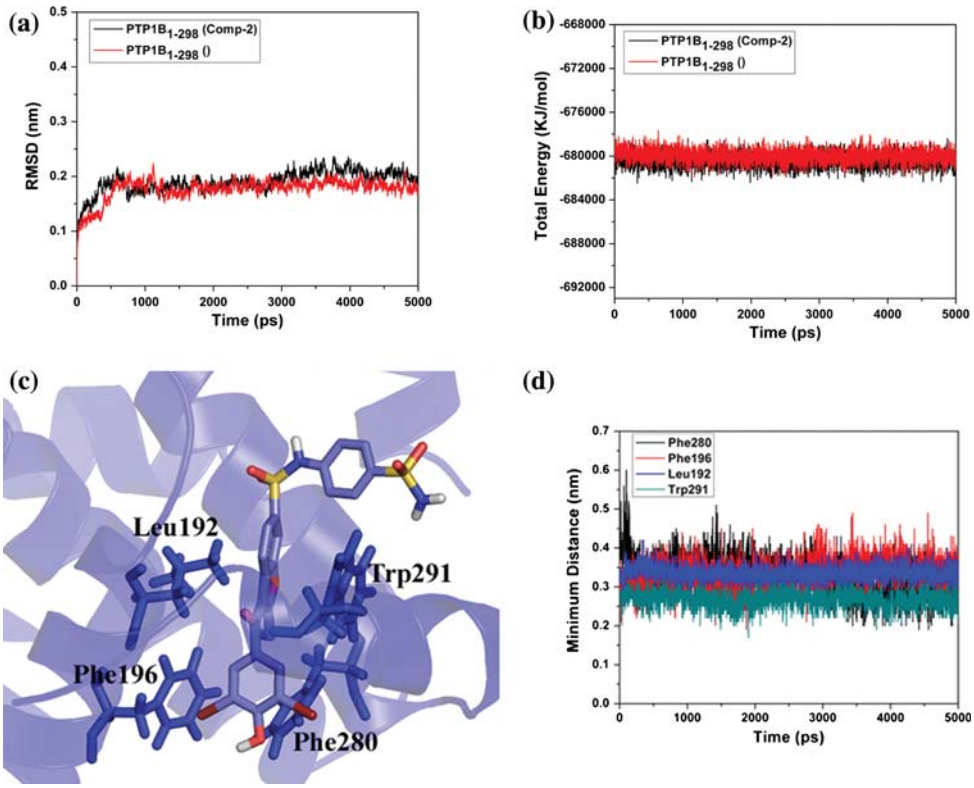

Fig. 1 RMSD with reference to initial structure (**a**) and total energy (**b**) for the 5 ns MD simulation of $PTP1B_{1–298}$ in the presence and absence of compound-2. The orientation of the hydrophobic residues shown as sticks around compound-2 in the final snapshot of MD simulation (**c**). The minimum distance between the compound-2 and the hydrophobic residues (Phe196, Phe280, Leu192, Trp291) are plotted throughout the 5 ns MD simulation (**d**)

the absence and presence of the allosteric inhibitor with respect to the initial conformation (Fig. 2c and d). The Glu200–Met282 distance relative to the initial structure is fluctuating within 0.2 nm while Glu200–Val287 is around 0.6 nm in the presence of allosteric inhibitor. In the absence of compound-2, such movement was not observed as the Glu200–Met282 and Glu200–Val287 distance, relative to the initial structure was fluctuating within 0.2 nm. From the above results it can be speculated that the allosteric inhibitor induced conformation of $PTP1B_{1–298}$ in which the α7 is propelled 0.6 nm upward can be the orientation of α7 helix in the open form or it might be a transition state between the closed and the open forms.

In the initial conformation of MD simulation, two H-bonds were observed between the compound–2 and the allosteric site of the protein (Fig. 3a). The two H-bonds were formed by the carbonyl group and the sulfonamide amino group of compound-2. The carbonyl group initially forms H-bond with the side chain of Asn193 but it soon establishes new H-bond with Ser295 leaving the Asn193 (Fig. 3b). This result motivated us to investigate whether such a change was genuine or a result of artifact. On surveying the $PTP1B_{1–298}$ crystal structures in closed form, it was evident that the Ser295 forms extensive H-bonds with α3 helix. It was also recently established that the mutation of Ser295 causes disruption of α7 interaction with the rest of the enzyme core [18]. Accordingly, in our simulation studies, although the Ser295 initially formed extensive H-bonds with α3, it is observed that the serine has gradually lost all its interactions with α3 and has formed with the allosteric inhibitor. Figure 3c illustrates the distance measured between the oxygen of compound-2 carbonyl group and the Ser295 hydroxyl and the hydrogens of side chain amino group of Asn193. The formation of new H-bond between the Ser295 and the allosteric inhibitor eliminates the interaction of α7 with the enzyme core. This result was further established when similar outcome was observed after repeating the same simulation ($PTP1B_{1–298}$ with allosteric inhibitor) with different initial velocities. In the absence of allosteric inhibitor, Ser295 is forming all the H-bonds with α3 throughout the simulation (data not shown). Therefore it is evident that the allosteric inhibitor is indeed preventing the α3–α6–α7 interaction pattern which is necessary for PTP1B to be in the closed form. The second H-bond formed between the sulfonamide amino and the carboxyl group of Glu276 is maintained during the entire simulation time and interestingly, Ser187 which is at the end of the WPD-loop leading into α6 is also forming H-bond with the sulfonamide amino group (Fig. 3d). Overall, our MD simulation studies of PTP1B protein in the presence and absence of allosteric inhibitor has provided new insights into the proposed mechanism of allosteric inhibition in stabilizing the open/inactive conformation.

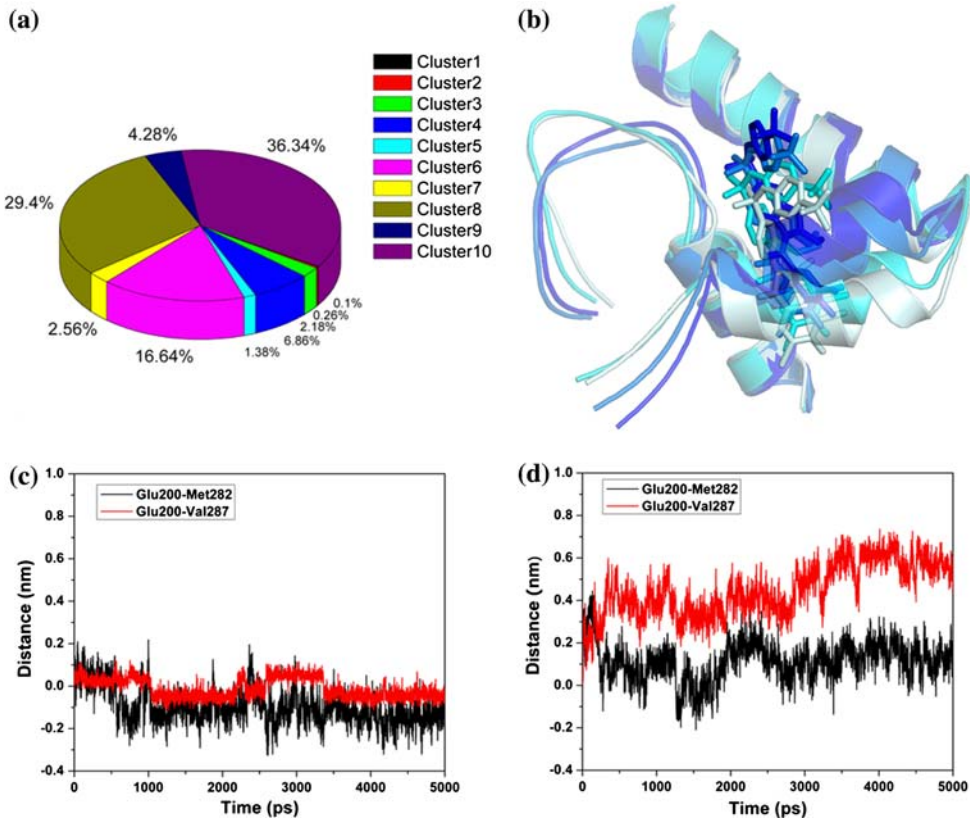

Fig. 2 The pie chart obtained from the cluster analysis of 5 ns conformational space of $PT1B_{1-298}$ with compound-2 shows ten clusters represented by different colors and the percentage of conformers in each cluster (**a**). The superimposition of four cluster representative structures of cluster 1 (light cyan), cluster 3 (cyan), cluster 6 (blue) & cluster 10 (dark blue) structures (**b**). The distance between α3–α7 was measured in the absence (**c**) and presence (**d**) of compound-2 for the entire simulation

Receptor based pharmacophore model generation

Another aim of this work was to develop reliable receptor based pharmacophore model for the allosteric site because an ideal model is very critical to search new lead/inhibitor candidate molecules. As the PTP1B-allosteric inhibitor complex crystal structure lacks α7, the 5 ns MD simulation with compound-2 can be the rational choice as it would take account of both $PTP1B_{1-298}$ and ligand flexibility at the allosteric site. In the protein conformation sampling procedure, we introduced a new method wherein instead of traditional random sampling from the thousands of MD snapshots, we utilized our cluster analysis results. From a total of ten clusters, the population of top three clusters (cluster 10, 8, and 6) represents 82.38% of total conformations (Fig. 2a). The cluster representative structures obtained from the large populated clusters will be suitable to represent the conformational space. Therefore, among the ten cluster representative structures, three will represent the entire MD simulation snapshots. The pharmacophore feature mapping for the compound-2 were performed for each of the three representative structures individually by considering HBD, HBA, RA, and HY features. Numerous features were obtained due to the consideration of the direction of each feature, but specific features were selected depending on the direction in which the compound-2 formed interactions with the protein (Fig. 4a). Therefore final receptor based pharmacophore model contained six features: one HBA, one HBD, three RAs and one HY. The HBA feature refers to the carbonyl group; HBD refers to sulfonamide amino group; the three RA refers to the benzofuran core, the dibromo phenol group and the ring of phenylsulfonamide groups respectively; and the HY feature refers to the ethyl group. Although four or five featured pharmacophore models are much preferable as they can retrieve more hits from databases, selection of six featured pharmacophore model was inevitable as all the crucial features responsible for binding, had to be considered. These features were selected based on the crystallographic and MD simulation results which have confirmed their crucial role in the binding of compound-2 to the protein.

Finally, three receptor based pharmacophore models (CLU10HYPO, CLU8HYPO and CLU6HYPO) with each six features were obtained representing the protein's and ligand's flexibility (Fig. 4b). If we merge these three receptor based pharmacophore models into one, it can be called "dynamic" pharmacophore model but instead we have taken the three pharmacophore models individually as each represents thousands of conformations which in turn considers the flexibility of protein structure. The mapping of the compound-2 onto CLU10HYPO demonstrates the features that have been responsible for its binding at the allosteric site (Fig. 4c). Validation of the pharmacophore model was carried out by mapping the CLU10HYPO onto

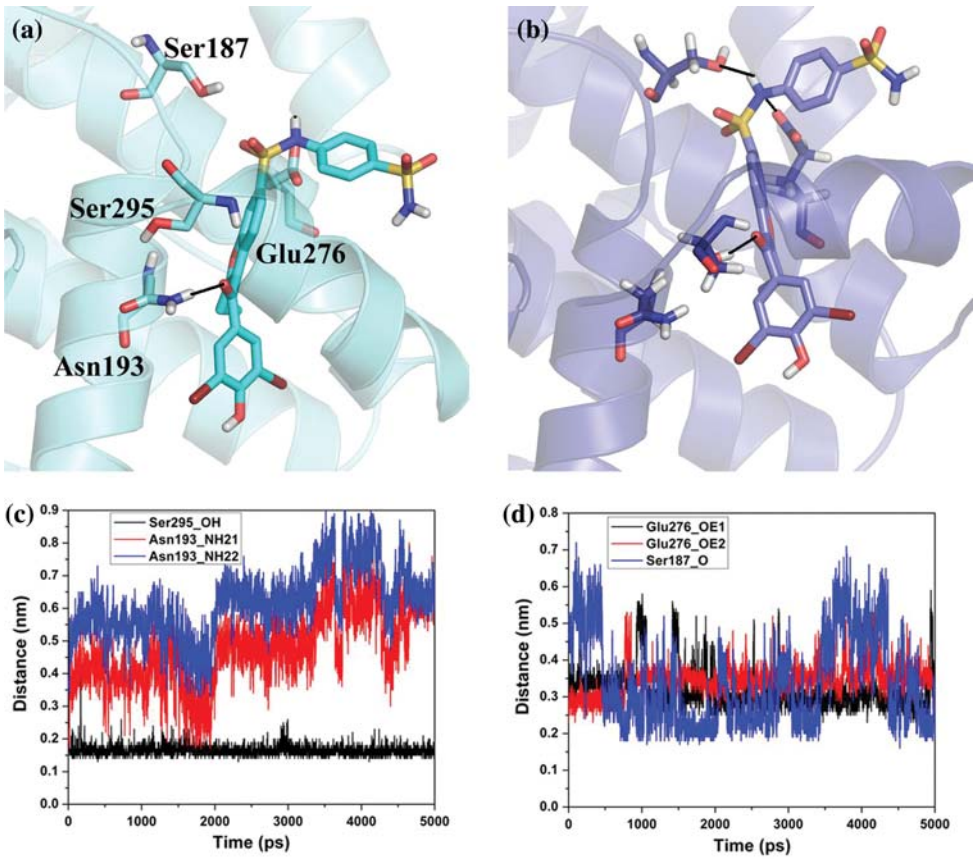

Fig. 3 Ribbon diagrams of initial (**a**) and cluster 10 representative structure (**b**) snapshots of $PTP1B_{1–298}$ with compound-2 represented in sticks showing its relative orientation with the crucial H-bonding residues. The distance between the intermolecular H-bonding atoms were measured throughout the 5 ns simulation (**c** and **d**)

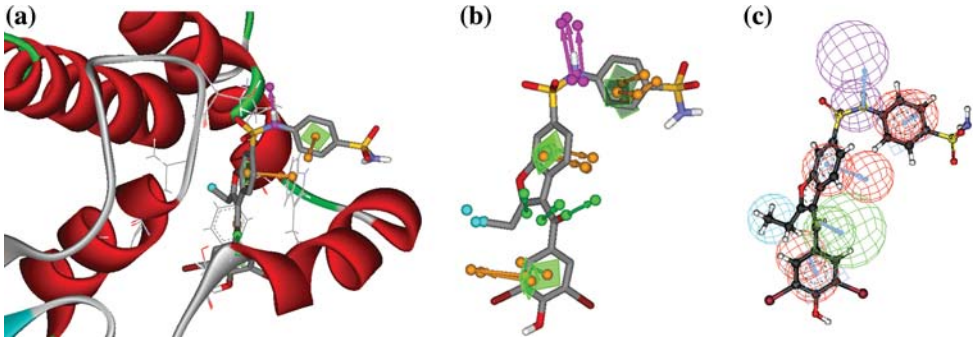

Fig. 4 The receptor based pharmacophore feature mapping of compound-2 (shown as sticks) from cluster 10 representative structure (shown as ribbons) (**a**). Overlapping of three hypothesis models, CLU6HYPO, CLU8HYPO and CLU10HYPO onto compound-2 (**b**). Mapping of compound-2 by CLU10HYPO (**c**)

two experimentally proved active compounds, compound-1and compound-3 with IC_{50} 350 μM and 8 μM respectively [14] (Fig. 8c and f of supplementary data). The crucial features of compound-1 were well mapped except for HBD and RA features. This is due to the lack of the amino and the benzenesulfonamide groups which are present in compound-2. In the case of compound-3, all the features were mapped perfectly. The chemical structures of compound-1 and compound-3 are shown in Fig. 9 of supplementary data.

Each CLUHYPO pharmacophore model was used for screening NCI2000 and Maybridge databases containing approximately 250,000 and 58,000 compounds, respectively. CLU10HYPO retrieved 2125 and 780 compounds while CLU8HYPO retrieved 1708 and 544 compounds and CLU6HYPO retrieved 1799 and 641 compounds from NCI2000 and Maybridge databases, respectively. Filtering of molecules based on certain properties such as molecular weight (≤500) and number of rotatable bonds (≤10) which could be calculated by catalyst program was utilized to eliminate compounds that did not possess physicochemical properties [28]. Further, compounds with a fit value ≥4 were considered for further evaluation. Hence, in total 152 and 133 unique compounds were obtained from NCI2000 and Maybridge databases, respectively.

Receptor based pharmacophore model validation by molecular docking studies

Molecular docking studies [29, 30] were performed to evaluate the molecules obtained from receptor based pharmacophore model screening and to examine their binding orientation at the allosteric site. Generally, docking would be done in one conformation (mostly crystal/modeled structure), but in our case apparent conformational change was observed in α7 orientation from MD simulation results. Therefore, it would be more appropriate to dock the 285 molecules into two different protein conformations, i.e., the initial structure and the structure representing cluster 10 to account protein flexibility. Initially, compound-2 was docked and compared with the binding conformations in crystal and cluster 10 representative structures for validation purpose. It can be observed that the docking simulation results have been successful in generating the correct conformations of the ligands at the allosteric site (Fig. 5). In the initial conformation, the carbonyl group of compound-2 interacts through H-bond with the side chain of Asn193, the NH group of sulfonamide group interacts with the carboxyl group of Glu276. In the cluster 10 representative conformation, the carbonyl group of compound-2 interacts with the hydroxyl group of Ser295 unlike the initial structure, but the NH group in sulfonamide group interacts with the Glu276 carboxyl side chain. In both conformations benzofuran ring tightly stacks with the Trp291 and Leu192 residues (Fig. 3 and 5). Further validation was performed by docking compound-1 and compound-3 which are also proven as PTP1B allosteric inhibitors. These two compounds also formed similar type of interactions at the allosteric site of $PTP1B_{1–298}$ (Fig. 8a, b, d and e in supplementary data).

The consideration for selecting molecular docked poses for further analyses was done based on the ligand conformations which (i) can satisfy the required interactions with protein and (ii) have reasonable goldscore. Finally, twelve Maybridge and eleven NCI2000 database molecules have shown the desired interactions with PTP1B and also have good goldscore. Among them, most of the molecular structures which have good goldscore (Fig. 6) are observed to have similar scaffold with compound-2. Among 25 hits found in the screening, RJF01044 and SPB00951 have been represented to show the interactions similar to compound-2. The carbonyl oxygen of amide group in RJF01044 and SPB00951 interacts with Asn193 in initial conformation while it interacts with Ser295 in cluster 10 representative conformation similar to compound-2. The NH group of the sulfonamide group interacts with Glu276 carboxyl side chain in both initial and cluster 10 representative conformations. In both compounds the phenyl moiety present between amide and sulfonamide groups tightly forms hydrophobic interactions with Trp291 and Leu192 like benzofuron in compound-2 (Fig. 7a, b, d, and e). The molecules were mapped onto the pharmacophore models revealing the features of the molecules that are responsible for interacting with PTP1B allosteric site (Fig. 7c and f). The orientation and the mapping of new compounds were similar to that of compound-2 (Fig. 4c). Therefore molecular docking studies have played a vital role in determining the compounds orientation at the binding site and also were useful in validating our pharmacophore models. Identifying new compounds based on receptor based pharmacophore modeling and validating them by docking in different conformations rather than one can be more reliable process in drug discovery process.

Conclusions

The MD simulation study of $PTP1B_{1–298}$ with allosteric inhibitor has revealed new insights into its allosteric inhibition mechanism. The α7 helix from closed form $PTP1B_{1–298}$ was modeled to the $PTP1B_{1–282}$ in open form. It has undergone certain changes in its orientation with respect to α3–α6 during the simulation time. It was interesting to note that, although Ser295 initially interacted with α3 helix with extensive H-bond network (through Asn193),

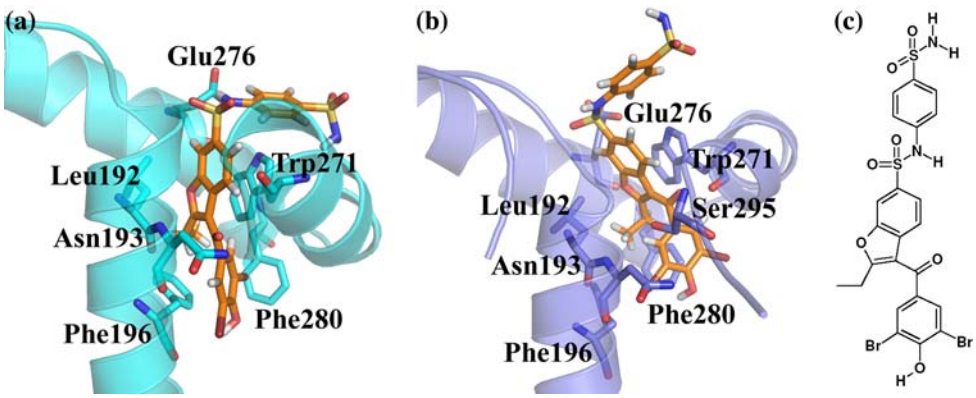

Fig. 5 Docking conformation of compound-2 in the initial structure (**a**) and cluster 10 representative structure (**b**). Molecular structure of compound-2 (**c**)

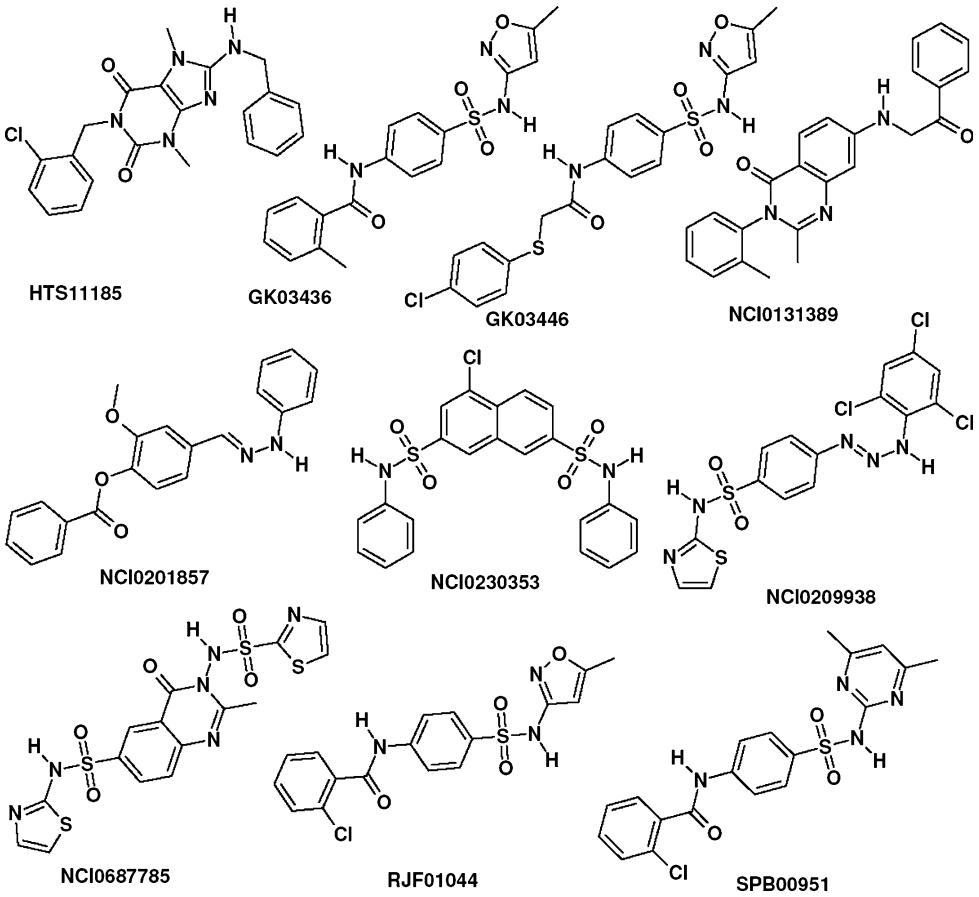

Fig. 6 The molecular structures of the hits obtained from NCI2000 and Maybridge databases by screening CLU10HYPO, CLU8HYPO and CLU10HYPO. These compounds have mol. wt. $\leq$ 500, rotatable bonds $\leq$10, best fit $\leq$ 4, and good goldscores

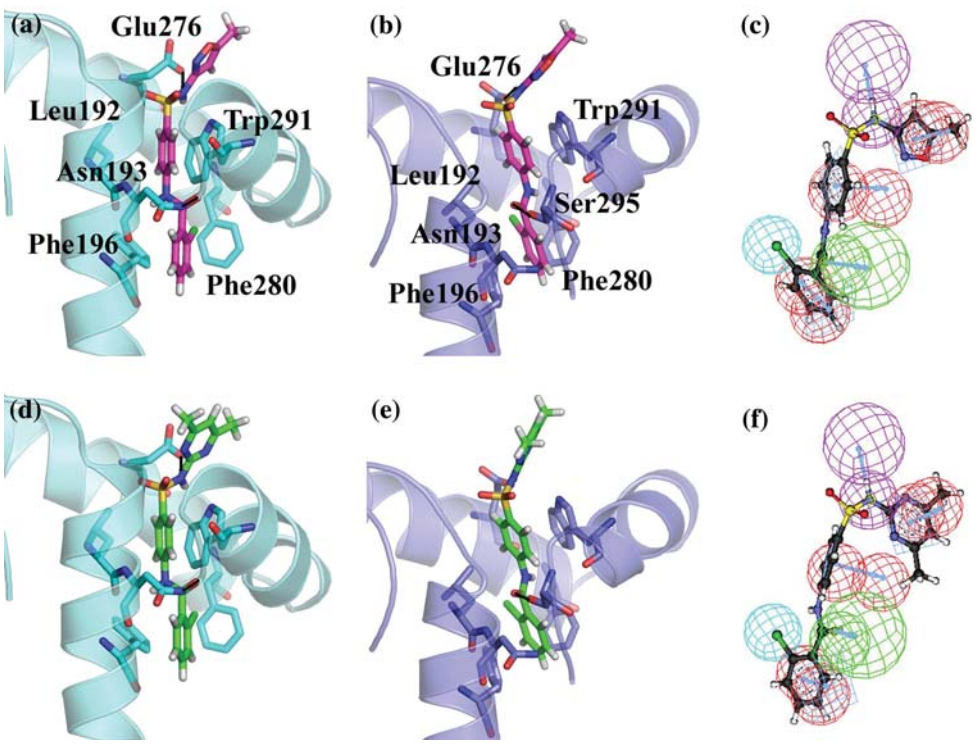

Fig. 7 Docking conformations of new compounds, RJF01044 (mageta) and SPB00951 (green) in the initial structure (**a** and **d**) and cluster 10 representative structure (**b** and **d**). The mapping of new compounds onto CLU10HYPO (**c** and **f**) respectively. The allosteric site is represented by α3, α6, α7 shown as ribbons and the interacting residues are shown as sticks

those interactions were gradually diminished and Ser295 formed new H-bond interactions with the carbonyl group of the allosteric inhibitor. On the contrary, the Ser295 strongly interacts with α3 helix in the absence of compound-2 throughout the simulation time. Together with our results and an earlier report stating that the mutation of Ser295 separates α7 hekix from the core protein indeed points us the important role of Ser295 in allosteric inhibition. Interestingly, the clustering analysis was helpful in viewing the upward movement of α7 helix around 0.6 nm with respect to α3–α6 helices. This has led us to speculate that the α7 helix orientation of cluster 10 representative structure might be its orientation in open form or might be in the transition state between the closed and the open forms. Overall, the loss of interaction of α7 from the core protein in the presence of allosteric inhibitor substantiates the hypothesis of Wiesmann et al. and also revealed certain clues on PTP1B allosteric inhibition.

Developing receptor based pharmacophore models for $PTP1B_{1–298}$ would be appropriate as allosteric inhibitors interact with α7, α6 and α3 helices. As the crystal structure lacks α7, the simulation of $PTP1B_{1–298}$ with compound-2 was considered and the cluster analysis representative structures were appropriate for our studies. Among ten cluster representative structures, three (CLU10HYPO, CLU8HYPO, CLU6HYPO) were selected as they represented maximum conformational space. A unique approach was implemented wherein the three individual pharmacophore models rather than one merged dynamic pharmacophore model was used for screening databases. New hits containing the features that complement the allosteric site were retrieved. These hits were filtered based on molecular weight and number of rotatable bonds and were docked into $PTP1B_{1–298}$ allosteric site. Two conformations were used for docking simulations as there was discernable transition in the α7 orientation with respect to α6–α3 helices. The final hits have structural and conformational similarity with existing PTP1B allosteric inhibitors. This methodology of analyzing the dynamic motion of the protein, then developing receptor based pharmacophore models to retrieve hits and finally performing docking into plausible conformations would be a reliable procedure to apply in identifying new lead molecules.

Acknowledgements Kavitha Bharatham and Nagakumar Bharatham were recipients of fellowships from the BK21 Programs and this work was supported by grants from the MOST/KOSEF for the Environmental Biotechnology National Core Research Center (grant #:R15-2003-012-02001-0).

References

1. Cicirelli MF, Tonks NK, Diltz CD, Weiel JE, Fischer EH, Krebs EG (1990) Proc Natl Acad Sci USA 87:5514. doi:10.1073/pnas.87.14.5514
2. Ahmad F, Li PM, Meyerovitch J, Goldstein BJ (1995) J Biol Chem 270:20503. doi:10.1074/jbc.270.35.20503
3. Johnson TO, Ermolieff J, Jirousek MR (2002) Nat Rev Drug Discov 1:696. doi:10.1038/nrd895
4. Zabolotny JM, Bence-Hanulec KK, Stricker-Krongrad A, Haj F, Wang Y, Minokoshi Y et al (2002) Dev Cell 2:489. doi:10.1016/S1534-5807(02)00148-X
5. Elchebly M, Payette P, Michaliszyn E, Cromlish W, Collins S, Loy AL et al (1999) Science 283:1544. doi:10.1126/science.283.5407.1544
6. Hooft van Huijsduijnen R, Sauer WH, Bombrun A, Swinnen D (2004) J Med Chem 47:4142. doi:10.1021/jm030629n
7. Frangioni JV, Beahm PH, Shifrin V, Jost CA, Neel BJ (1992) Cell 68:545. doi:10.1016/0092-8674(92)90190-N
8. Iversen LF, Moller KB, Pedersen AK, Peters GH, Petersen AS, Andersen HS et al (2002) J Biol Chem 277:19982. doi:10.1074/jbc.M200567200
9. Asante-Appiah E, Ball K, Bateman K, Skorey K, Friesen R, Desponts C et al (2001) J Biol Chem 276:26036. doi:10.1074/jbc.M011697200
10. Sun JP, Fedorov AA, Lee SY, Guo XL, Shen Lawrence DS, Almo SC et al (2003) J Biol Chem 278:12406. doi:10.1074/jbc.M212491200
11. Puius YA, Zhao Y, Sullivan M, Lawrence DS, Almo SC, Zhang ZY (1997) Proc Natl Acd Sci 94:13420. doi:10.1073/pnas.94.25.13420
12. Asante-Appiah E, Patel S, Desponts C, Taylor JM, Lau C, Dufresne C et al (2006) J Biol Chem 281:8010. doi:10.1074/jbc.M511827200
13. Wrobel J, Sredy J, Moxham C, Dietrich A, Li Z, Sawicki DR et al (1999) J Med Chem 42:3199. doi:10.1021/jm990260v
14. Wiesmann C, Barr KJ, Kung J, Zhu J, Erlanson DA, Shen W et al (2004) Nat Struct Mol Biol 11:730. doi:10.1038/nsmb803
15. Barford D, Flint AJ, Tonks NK (1994) Science 263:1397. doi:10.1126/science.8128219
16. Jia Z, Barford D, Flint AJ, Tonks NK (1995) Science 268:1754. doi:10.1126/science.7540771
17. Kolmodin K, Aqvist J (2001) FEBS Lett 498:208. doi:10.1016/S0014-5793(01)02479-6
18. Montalibet J, Skorey K, McKay D, Scapin G, Asante-Appiah E, Kennedy B (2006) J Biol Chem 281:5258. doi:10.1074/jbc.M511546200
19. Kamerlin KCL, Rucker R, Boresch S (2006) Biochem Biophys Res Commun 345:1161. doi:10.1016/j.bbrc.2006.04.181
20. Kamerlin KCL, Rucker R, Boresch S (2007) Biochem Biophys Res Commun 356:1011. doi:10.1016/j.bbrc.2007.03.093
21. Deng J, Lee KW, Sanchez T, Cui M, Neamati N, Briggs JM (2005) J Med Chem 48:1496. doi:10.1021/jm049410e
22. Berendsen HJC, van der Spoel D, van Drunen R (1995) Comput Phys Commun 91:43. doi:10.1016/0010-4655(95)00042-E
23. van der Spoel D, Lindahl E, Hess B, van Buuren AR, Apol E, Meulenhoff PJ, et al (2005) Gromacs User Manual version 3.3, http://www.gromacs.org
24. Schuettelkopf AW, van Aalten DMF (2004) Acta Crystallogr D Biol Crystallogr 60:1355. doi:10.1107/S0907444904011679
25. Discovery Studio 1.7, Accelrys Inc., San Diego, CA, USA
26. CATALYST 4.11, Accelrys Inc., San Diego, CA, USA
27. Jones G, Willett P, Glen RC, Leach AR, Taylor R (1997) J Mol Biol 267:727. doi:10.1006/jmbi.1996.0897
28. Bharatham N, Bharatham K, Lee KW (2007) J Mol Graph Model 25:813. doi:10.1016/j.jmgm.2006.08.002
29. Bharatham N, Bharatham K, Lee KW (2007) Arch Pharm Res 30:533
30. Bharatham K, Bharatham N, Park KH, Lee KW (2008) J Mol Graph Model 26:1202. doi:10.1016/j.jmgm.2007.11.002